Noncontact Determination of Velocity and Volume of Nanoliter Droplets on the Fly

Andreas Ernst, Lin Ju, Bernhard Vondenbusch, Roland Zengerle, and Peter Koltay

***Abstract*—We present a sensor for measuring volume and velocity of dispensed nanoliter droplets in a noncontact manner on the fly. The sensor-setup has a total thickness of 3.2 mm and can easily be mounted underneath any given nanoliter dispenser for continuous online monitoring of its dispensing performance. The principle is based on the interaction of dispensed single droplets of sample liquid passing the electric field of an open plate capacitor. The effect depends on droplet parameters like volume, velocity, and dielectric constant and is discussed in the paper. The presented data analysis enables a velocity independent volume determination of water droplets in the range from 26 to 82 nl with an accuracy of 3 nl. The sensor signal is sensitive to the alignment of the flight path of the nanoliter droplets within the 1.2-mm wide open capacitor and can lead to systematic volume errors of up to $\Delta V \sim 12$ nl. The impact of different dielectric constants can only be differentiated for very high variations; thus, the sensor needs to be calibrated to the different types of liquids.**

***Index Terms*—Capacitive sensor, noncontact volume determination, nanoliter dispensing, process control.**

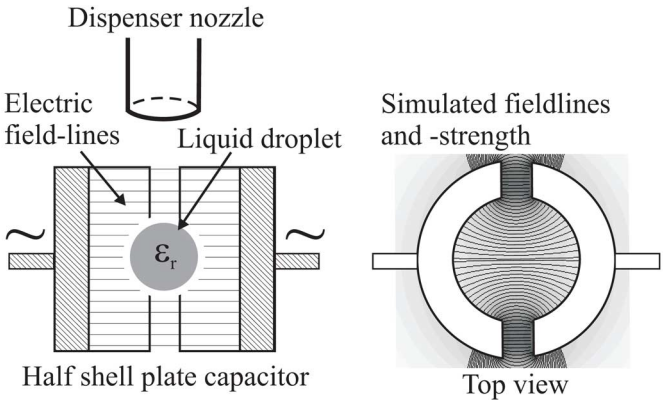

Fig. 1. Principle sketch of the capacitive measurement concept; a droplet passes through the electric field of the half shell plate capacitor. The "Top view" image visualizes a FEM simulation of the shape and strength of the electric field for the specific half shell electrodes. The gray background indicates for the field strength.

I. Introduction

THE selective application of well defined aliquots of liquid in the pico- to nanoliter range has received increasing interest in various applications in the past years [1]. The highly precise dosage of small amounts of chemical reagents is required in the field of pharmaceutical research, combinatorial chemistry as well as for the accurate delivery of lubricants or cooling agents for certain industrial processes. Often contactless dispensing systems are applied to deliver sample liquids as single, free flying droplets with precisely defined volumes at a high spatial resolution.

Such dispensing devices often require process control systems to evaluate the stability and performance of the dispensing process, because malfunctions due to clogging or nozzle wetting are quite common. Various methods to monitor a dispensing process and to measure droplet volumes have been reported, e.g., high-precision gravimetric balances or stroboscopic imaging systems [2]. Drawbacks of these commercially available systems are high cost and mostly big size. Furthermore, the loss or contamination of sample liquid can often not be avoided, if the control system requires contact to the dispensed liquid to perform the measurement (e.g., balance).

The capacitive droplet sensor presented in this work is designed to overcome these limitations by its small size and its capability of being integrated with the dispenser setup without disturbing the dispensing process at a given application.

This sensor was already published in an earlier state of research in [5]. However, the sensor principle, fabrication and measurement setup is briefly reviewed in the following.

The novelty of the presented state of research is focused on the characterization of the sensor performance, including the study of several influence parameters, starting at V.

II. Detection Principle

The presented capacitive measurement method is sensitive to volume and dielectric constant of the media, which will be confirmed by the presented experiments throughout this paper. The basic principle is sketched in Fig. 1. A liquid droplet, introduced in between the electrodes of an open plate capacitor leads to an increase of the average capacity of the electrode arrangement. Theoretically, the change of capacity depends on the size of the present droplet and the dielectric constant of the dispensed liquid only

$$\Delta C = 4 \cdot \pi \cdot \varepsilon_0 \cdot \frac{{r_{\mathrm{droplet}}}^3}{s^{\cdot 2}} \cdot \frac{\varepsilon_r - 1}{\varepsilon_r + 2} \tag{1}$$

where ΔC is the average change of the measurement capacitor's capacity induced by a droplet, ε_0 the permittivity of the vacuum, s the distance of the capacitor electrodes, rdroplet the droplets radius, and ε_r the dielectric constant of the droplet's liquid. Equation (1) holds for exactly spherical shaped droplets

Manuscript received March 04, 2010; accepted November 14, 2010. Date of publication November 29, 2010; date of current version May 25, 2011. This work was supported by the Ministry of Science, Research, and Art of the Federal State of Baden-Württemberg, Germany. The associate editor coordinating the review of this paper and approving it for publication was Prof. Istvan Barsony.

A. Ernst, R. Zengerle, and P. Koltay are with the Laboratory for MEMS Applications, Department of Microsystem Engineering–IMTEK, University of Freiburg, 79110 Freiburg, Germany (e-mail: andreas.ernst@imtek.de; zengerle@imtek.de; koltay@imtek.de).

L. Ju and B. Vondenbusch are with the Department of Mechanical and Process Engineering, Hochschule Furtwangen University, 78054 Villingen-Schwenningen, Germany (e-mail: jl@hs-furtwangen.de; vdb@hs-furtwangen.de).

Digital Object Identifier 10.1109/JSEN.2010.2095837

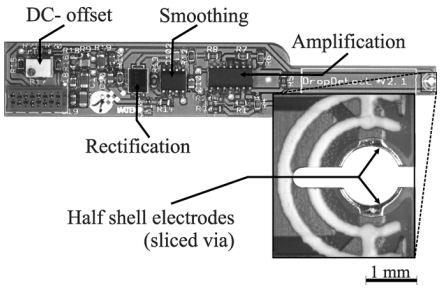

Fig. 2. Populated sensor PCB prototype V2.1 adapted to the PipeJet™ dispenser P18 [4]. The enlarged aspect visualizes the sensor capacitor consisting of a sliced standard through connection.

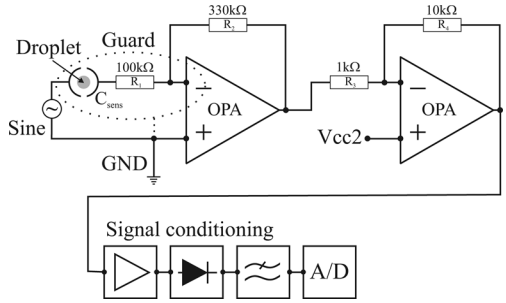

Fig. 3. Block diagram of the measurement chain. The detailed section shows the low impedance front end, indicating the simple connection of the guard to ground potential.

measured at stationary conditions with an open plane parallel plate capacitor.

However, in reality a dispensed droplet passes through the capacitor with a specific velocity and fluctuations in the droplets shape. Even long jets can occur, depending on the ejection characteristics of the specific liquid. Furthermore, the capacitor presented in this paper consists of two half shell electrodes and therefore (1) can only be considered as a first approximation.

III. Sensor Properties

The presented sensor is completely manufactured in standard PCB (printed circuit board) technology, which allows for an easy integration of the sensor capacitor at low cost fabrication of the whole sensor unit. The measurement capacitor is realized by a symmetrically separated standard through connection (via) featuring an inner diameter of $\mathrm{d} = 1.2$ mm. Therefore, two half shell electrodes are created, which enable droplets, with volumes in the range from ($\mathrm{V_{drop}} = \{5 - 120\ \mathrm{nl}\} \leftrightarrow \mathrm{d_{drop}} = \{212 - 612\ \mu\mathrm{m}\}$), to pass through; see Fig. 2. An advantage of the use of half shell electrodes is the specific shape of the electric field (see Fig. 1), which increases the sensitivity to changes in capacitance caused by a droplet [3]. This is an essential detail which enables to measure the very small droplets with a comparably large capacitor.

The electrical transformation of the changes in capacitance to significant, interpretable voltage signals is implemented by a low impedance front end of an inverting high-pass filter, modulated by a measurement sine frequency of $\mathrm{f} = 160$ kHz at $\mathrm{U_{pp}} = 20$ V; see Fig. 3. An induced droplet in between the electrodes leads to an increase of the average capacitance of the measurement capacitor, which goes along with a shift in the gain-response of the filter. Thus, the amplitude of the front end output voltage will follow the capacitive change proportionally.

The generated signals are further conditioned by two successive amplification steps followed by an adapted rectification and smoothing. For more details on this see [5].

Another important feature to improve the accuracy of the measurement of small capacitive alternations is the so called "guard-ring" technology. A guard-ring in form of a third electrode, which surrounds the front end, protects the measurement chain from the influence of occurring bulk- and surface leakage currents. An attractive advantage, provided by the used low impedance front end is the virtual connection to ground potential. It allows for a passive guarding to ground by the connection of the guard to ground potential of the circuitry [6], [7]. Therefore, it is possible to use an extensive ground area, which covers the whole sensor PCB as guard-ring. Furthermore, the complete aluminum housing of the used dispensing system is connected to the guard; thus, the analog circuit is protected from the influence of the high-voltage piezo actuation of the used dispenser; see Section IV.

IV. Measurement Setup

The complete measurement setup to perform the presented experiments, described in the following, consisted of a PipeJet™ P18 dispenser module from BioFluidix GmbH [8], combined with an adapted sensor support and the sensor PCB prototype shown in Fig. 2. The dispenser features a nozzle diameter of $\mathrm{d_{nozzle}} = 500\ \mu$m with a distance to the capacitor of $\mathrm{h} = 1.4$ mm, defined by the support.

A precise evaluation of the presented sensor requires a reliable correlation of the analog sensor signals to the corresponding droplets' volumes and flight characteristics. The precise volume determination of single dispensed droplets in the target volume range is realized by a high precision gravimetric balance from Sartorius (SC2), which was installed below the dispenser–sensor arrangement. Thus, each dispensed droplet can be monitored by the sensor before it impinges on the balance. A stroboscopic camera completes the setup, which enables to image the droplet's characteristics like shape fluctuations and velocity with respect to the dispensing parameters. The whole setup was installed on a vibration cushioned table and shielded by a wind shield cover to prevent environmental influence. Fig. 4 provides a sketch of the complete setup.

The PipeJet™ dispenser technology is based on a piezo-electric actuator to generate free-flying droplets in the nanoliter range. A brass piston, driven by the piezo-electric stack, squeezes a liquid filled elastic polymer micro tube. Therefore, the inner volume of the tube becomes reduced, and the displaced liquid is forced to move into the direction of the dispenser nozzle (outlet) as well as back into the liquid reservoir (inlet). Due to the fluidic resistance ratio from the displacement area to the outlet nozzle versus from the displacement area to the inlet reservoir, a well-defined fraction of liquid is ejected out of the nozzle as free flying droplet almost independent on liquid viscosity. The volume and velocity of the dispensed

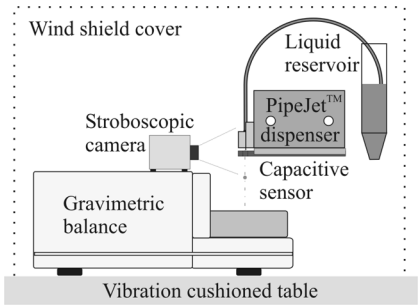

Fig. 4. Principle sketch of the complete measurement setup, used for the characterization of the sensor performance.

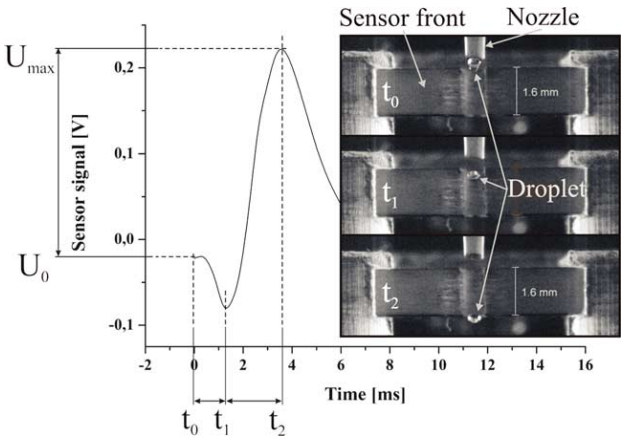

Fig. 5. Typical sensor signal generated by a pure water droplet. The stroboscopic picture sequence correlates significant points in time to particular droplet positions in the sensor capacitor. The shown images are recorded from earlier experiments; thus, the distance from nozzle to sensor is different at the presented setup. The images are used for the visualization of the droplet positions only.

droplets can be adjusted by varying the extension length and extension velocity of the piezo-electric actuator [4].

V. Sensor Performance

In an earlier publication [5], the sensor setup was used for droplet presence detection only, without the capability of measuring the droplet volume or droplet velocity precisely. The previously investigations on the sensor signals, generated by pure water droplets, have shown a certain dependency of the sensor signal peak value to the causative droplet volume, which is studied and quantified in more detail in the following.

Fig. 5 presents a typical time dependent sensor signal correlated to certain droplet positions during a droplet's flight through the sensor capacitor. The signal correlation to the droplet positions was determined by comparing stroboscopic images at certain points in time to the generated signals [2].

The negative peak at the beginning of the signal (t_0 to t_1) indicates for an approaching liquid droplet. This voltage decrease might be explained by a capacitive coupling effect of a growing droplet via the liquid column inside the dispenser to GND potential. This entails a decrease of the charge on the measurement electrode, caused by the presence of the droplet, connected to the reservoir by the liquid column, before the droplet tears off. However, this aspect was not studied in greater detail yet.

The time interval from t_1 to t_2 is the time between a droplet's tear off from the nozzle, representing the disconnection from the liquid column, until it exits the capacitor. For the present set up, this gives an apposite estimate for the time of flight (ToF) of a droplet through the sensor capacitor. The increase in the signal amplitude to $\mathrm{U}_{\max}$ during this time interval is caused by the change in capacity induced by the presence of the droplet in between the capacitor electrodes. This increase continues until the droplet exits the capacitor, which is obviously based on the specific characteristics of the read out circuit. For $\mathrm{t} > \mathrm{t}_2$ the signal decays to its initial value with a certain time constant defined by the amplification circuit.

Quantitative studies on the signal characteristics have shown that the peak signal value is influenced by the droplet volume as well as by the droplet velocity.

The linear coherence of these values was experimentally found and is described in more detail in [9].

Therefore, the peak signal value cannot be considered as primary sensor value alone, independently of the droplet's velocity.

Nevertheless, it has been found empirically that the droplet volume as function of the peak signal value and the droplet velocity can be described very well by the following equation:

$$V_{\mathrm{droplet}} = C_1 \cdot U_{\max} + C_2 \cdot u_{\mathrm{droplet}} + C_3 \tag{2}$$

where $\mathrm{U}_{\max}$ is the signal peak value and u_{droplet} the droplet's velocity. The factors C_1 to C_3 are necessary values to calibrate the sensor performance to standard reference measures for the droplet volumes. Equation (2) thus enables the determination of the droplet volume directly from the sensor signal. However, in order to be able to apply (2) for calculation of the droplet volume the calibration constants C_1 to C_3 have to be determined by a calibration experiment first. Further, for every measurement the signal peak values, defined by U_0 to $\mathrm{U}_{\max}$ (see Fig. 5) as well as the droplet velocity have to be inserted to be able to apply (2) correctly.

The signal peak value can be determined straight forward form the analog signal by simple peak detection methods. The velocity of the droplet u_{droplet} however remains unknown in first instance, but it turns out that an essential feature of the presented setup is the ability to estimate the droplet velocity directly from the generated analog signals like described and validated in the following.

A. Droplet Velocity Estimation

The droplet velocity is defined by a certain distance which the droplet transmits at a specific time interval. A droplet specific time interval is given by the ToF, which the droplet needs to pass through the sensor. An inverse relation of ToF to the corresponding transmitted distance, defined by the sensor capacitor height (here $\mathrm{s} = 1.6$ mm), gives a simple estimate for the droplet's velocity. Therefore, the droplet velocity can be calculated by the following equation:

$$u_{\mathrm{droplet}} \approx \frac{s}{t_2 - t_1}. \tag{3}$$

For an experimental validation of (3) the estimated results of u_{droplet} according to (3) were correlated to standard reference

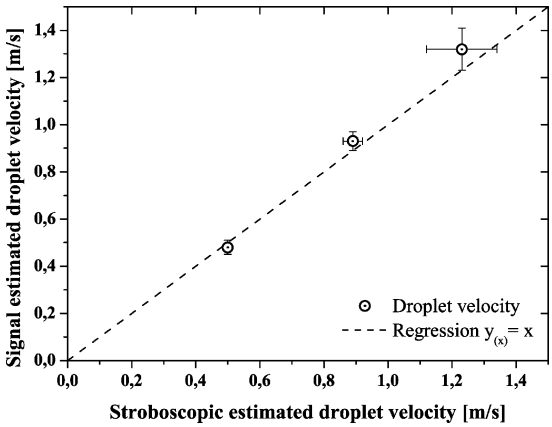

Fig. 6. Correlation of the stroboscopic estimated droplet velocities versus the signal extracted droplet velocities.

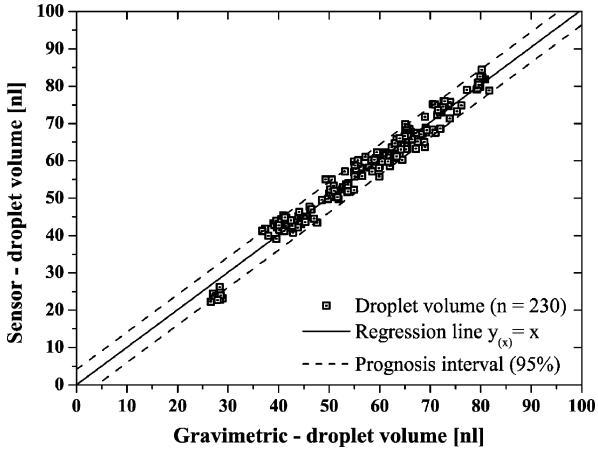

Fig. 7. Correlation of the gravimetrically determined droplet volumes (standard reference) to the volumes calculated according to (2) by the sensor generated signals. The gray line serves as guideline ($y_{(x)} = x$) and does not represent a linear fit of the results!

measurements for the droplet velocity, based on stroboscopic image sequences.

Therefore, several images of one stroboscopic recorded droplet sequence were evaluated with respect to the distance, covered by the shown droplet. Thus, the droplet velocity can be calculated by

$$u_{\mathrm{Strobo}} = \frac{d_{\mathrm{drop}}}{\Delta t \cdot (n_{\mathrm{image}} - 1)} \tag{4}$$

where $\mathrm{d_{drop}}$ is the distance [m] which the droplet covered, identified by the images, Δt [s] is the time shift in between the individual images and n indicates for the number of images of the used sequence.

Droplet velocities, calculated according to (4) were used as validation reference and depict on the x-axis in Fig. 6. The error for this measurement was estimated by the size of the blur surrounding the droplet image. Additionally, a time error of $\Delta \mathrm{t} = 0.1$ ms was considered as measurement uncertainty due to the shutter time of the used camera [10]. The errors depict on the y–axis, arise from the standard deviation, applying (3) to 40 individual measurements for each velocity regime, respectively. The results of the validation experiment are shown in Fig. 6, illustrating the resulting error bars.

Fig. 6 shows a diagram of the droplet velocity estimated directly from the sensor signal according to (3) correlated to the stroboscopic measured droplet velocity according to (4). The dashed line serves as guideline to the eye, indicating the regression $y_{(x)} = x$.

Obviously, (3) enables a quite accurate estimate of the droplet velocity in the range from 0.5 m/s to 1.2 m/s with an error of typically less than 0.1 m/s. Thus, velocity values determined from the analog signal according to (3) can be used as reasonable estimates of u_{droplet} to be inserted in (2).

B. Droplet Volume Measurement

To evaluate the sensor performance with respect to droplet volume, a previously performed experiment was reconsidered, where droplets of various size where dispensed at constant velocity of $u_{\mathrm{droplet}} = 0.7$ m/s; see [5]. It was found that the signal peak values correlate well with the corresponding droplet volume for droplets of constant velocity. More extensive investigations have shown that for different droplet velocity regimes the signal peak values correlate to the droplet volume as well, but feature specific regression slopes for each velocity.

In order to study the sensor performance regarding the droplet volume at variable droplet velocities, further experiments were accomplished where 230 single droplets of individual droplet volumes in the range from $\mathrm{V} = \{26 \text{ to } 82 \text{ nl}\}$ and individual droplet velocities from $u = \{0.17 \text{ to } 0.96 \text{ m/s}\}$ were measured by the described measurement set up (see Section IV).

The determination of the droplet volumes by the sensor according to (2) required the definition of the calibration factors $\mathrm{C_1}$ to $\mathrm{C_3}$ first. This was realized by applying standard multiple regression estimation to the experimentally gained set of signals, in correlation to the corresponding gravimetrically determined droplet volumes as reference. The acquired data set lead to the definition of the calibration factors like follows: $\mathrm{C_1} = 117.8$ nl/V, $\mathrm{C_2} = 29.8$ nls/m and $\mathrm{C_3} = -7.2$ nl.

Applying (2), including the described factors and droplets velocities, calculated by (3), enabled to determine single droplet volumes directly from the measured signals like shown in Fig. 7. Here the gravimetrically determined droplet volumes (x-axis) are compared to the volumes calculated according to (2) (y-axis). The certain parameters $U_{\max}$ and u_{droplet}, required for the application of (2) are directly determined from the generated analog sensor signals. The gray line serves again as guideline, depicting a 100% correlation, whereas the dashed lines indicate a calculated prognosis interval of 95% to estimate the error in volume accuracy of the measurement. The multiple regression estimation led to a standard deviation of $\sigma = 2.2$ nl and a correlation coefficient of $r_{(z,xy)} = 0.985$, whereas the maximum error, defined by the prognosis interval of 95%, is $\Delta \mathrm{V} = \pm 3$ nl.

C. Discussion on the Sensor Performance

The presented capacitive droplet sensor enables the contactless measurement of a variety of information about dispensed droplets in the nanoliter range at once, which can be determined directly from the sensor generated analog signals.

First, the droplet velocity can be estimated by correct signal interpretation with maximum error in accuracy of $\delta u_{\max} =$

$+0.1$ m/s and a maximum deviation in precision of $\Delta u = \pm 0.1$ m/s for the considered measurement range ($u_{\text{droplet}} < 1.3$ m/s). The results including the error bars are depicted in Fig. 6.

It can be seen that the application of (3) as well as the stroboscopic velocity estimation method (4) imply an increasing error for droplets at high velocity. This might derive from increasing droplet deformation caused by the required high dispensing dynamics to generate fast droplets with the used dispensing unit [4].

Having defined a droplet's velocity enables the application of (2) for the calculation of the droplet's volume. The derivation of this equation, based on standard multiple regression estimation, enables further the online determination of a dispensed droplet's volume with an accuracy of $\Delta \mathrm{V} = \pm 3$ nl, gained from the calibration measurement shown in Section V.

A validation of the defined calibration factors C_1 to C_3, will be given in the following Section VI, where the identical factors are applied to (2) to calculate the volumes of measured droplets of different solutions than pure water.

Theoretically, the capacitive measurement principle is sensitive to a variety of influence parameters, especially the dielectric constant ε_r of the liquid and the lateral droplet position in between the measurement capacitor. To study the influence of those parameters to the sensor performance several experiments where accomplished and described in the following to quantify those influence effects.

VI. Influence Parameters

A. Influence of the Dielectric Constant

One of the mentioned considerable influence factors, which derive from theory, is the dielectric constant ε_r of the droplets media. Equation (1) shows the dependency of the change in capacity due to a liquid droplet with dielectric constant ε_r by the Clausius–Mossotti factor $\mathrm{f}_{\varepsilon r}$:

$$f_{\varepsilon_r} = \left(\frac{\varepsilon_r - 1}{\varepsilon_r + 2}\right). \tag{5}$$

Obviously, the influence of changes in ε_r is smaller for liquids with large dielectric constants, given by the nonlinearity of the factor.

To relate the influence of variable dielectric constants on the sensor performance at constant conditions, several hundred droplets of liquid with different dielectric properties were dispensed through the sensor capacitor and analyzed by the application of (2), using the calibration factors determined for water in Section V.

To vary the dielectric constant of the liquid at mostly constant rheological properties, which is required to enable a constant droplet formation, saline solutions with different concentrations, were used for the measurements [11], [12].

To generate data at very low dielectric constants a nonpolar liquid (gear oil – SHC624, ExxonMobil) was also used for the experiments (see Table I). Such liquids, however, require different dispensing parameters compared to water solutions, which leads to extremely different droplet shapes, entailing further errors caused by droplet deformation.

TABLE I
Dielectric Constants for Different Saline Solutions (@ 20 °C; f < GHz) According to [12]

Solution	*Conc. [mol/l]*	*Dielectric constant ε_r @ 20°C*
Water	*pure (DI)*	*81*
Saline solution	*1.0*	*63*
Saline solution	*2.0*	*51*
Saline solution	*3.0*	*43*
Oil (SHC624)	*- - -*	*~ 2*

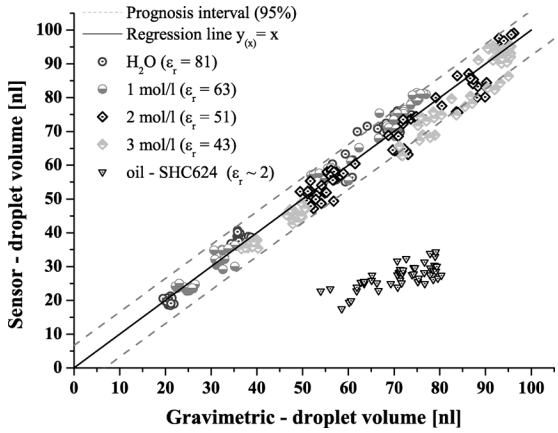

Fig. 8. Correlation of the sensor determined droplet volumes to the gravimetrically determined reference values for different solutions, indicated by the different symbols. The gray line serves as guideline ($y_{(x)} = x$) and is not a linear fit of the results!

The results of the experiment with water and saline solutions at identical velocities including the oil measurements featuring different droplet shapes and velocities are shown in Fig. 8.

Obviously a change of the dielectric constant in the range from 43 to 81—as provided by the saline solutions—does vary the correlation function only by around 3% and does not significantly falsify the droplet volume calculated by the sensor calibrated according to (2) to water as a reference medium. However, for a very small dielectric constant like for the gear oil, the change can be considerably and the sensor would need a recalibration to the specific properties.

B. Influence of Lateral Sensor Misalignment

The following section studies the influence of the position of the droplet's flight path with respect to the center of the sensor capacitor. Due to the theoretical assumption that the electric field in between the half shell electrodes is inhomogeneous—which was confirmed by an electric field simulation—see Fig. 1 and [5], each specific droplet position will introduce an error of certain magnitude to the measurement.

To estimate the size of such errors, five different droplet positions (a.–e.) were predefined, see Fig. 9, and the specific influence of the position was investigated by experiment.

Within the experiment droplets of a water-ink mixture were dispensed through the sensor capacitor at the various positions. A camera, installed below the sensor served to monitor the droplets position. The droplets impinged on a hydrophobic coated glass slide, which was mounted above the camera lens, after they had passed the sensor capacitor. The ink-mixture

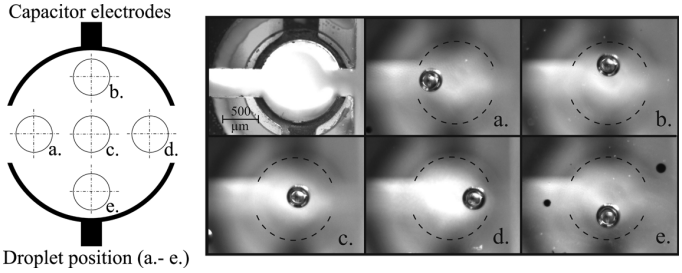

Fig. 9. Principle sketch of the target positions of the droplets (a.-e.) relative to the capacitor electrodes. The image sequence shows the realization of the position influence experiment. Single droplets were dispensed at the sketched positions through the sensor capacitor.

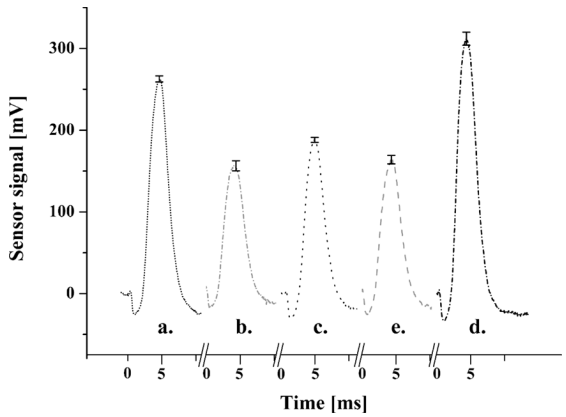

Fig. 10. Analog sensor signals gained from the experiments with different lateral sensor alignments. The individual signal peaks (a.-e.) are generated by droplets of the same volume and velocity dispensed at different lateral positions relative to the capacitor electrodes. Each peak is indicated by a letter to correlate the peak to the corresponding droplet position in Fig. 9.

was used to increase the contrast of the image. The actual measurement positions compared to the aspired positions are given by the picture sequence in Fig. 9. The diffuse images of the capacitor in the pictures a.–e. derive from the small focal depth of the camera. Therefore, a sharp image of the sensor, taken from the same position is provided in the left upper corner as reference. The dashed lines in the several pictures indicates the actually shape of the capacitor electrodes as guideline.

The images enable to correlate the generated analog sensor signals to the corresponding lateral droplet position in between the measurement capacitor. All droplets were dispensed with equal velocity and volume.

The mean value of ten sensor signals generated at the certain droplet positions are shown in Fig. 10. Each sensor signal represents a particular position (a.–e.). The statistical standard deviation of the individual peak values are given by the provided error bars.

C. Discussion on Influence Parameters

The discussed results, presented in Section V, represent the sensor performance at ideal boundary conditions. The experiments were accomplished using one droplet media (pure water) at an accurate alignment of the dispenser nozzle to the centre of the measurement capacitor, but these accurate results can be supposed to the influence of a set of certain influence parameters. One of these parameters is the dielectric constant of the measured media.

Theoretically, the dielectric constant has a non – linear influence to the change in the capacity, see (1). The results of the experiment from Section VI-A, however, have shown that the droplet's dielectric constant does not influence the sensor response for the considered range ($\varepsilon_r = 43$ to $\varepsilon_r = 81$) significantly. For this considered range the Clausius–Mossotti factor $f_{\varepsilon r}$, see (4), changes from 0.96 to 0.93 only. As very low dielectric reference, gear oil with $\varepsilon_r \sim 2$ was used, which results in a factor $f_{\varepsilon r}$ of 0.25. As expected, the experiments resulted in very low sensor peak signals and a significant different correlation to the reference; see Fig. 8. As a result from theory and experiment, the sensor can be considered nearly independent on the dielectric constant for a wide range of liquids, especially if the liquids with dielectric constants larger than approx. $\varepsilon_r = 30$.

The assumed error for the influence of variable dielectric constants in the range from $\varepsilon_r = 43-81$ is gained from the accomplished experiments and calculated by standard prognosis interval (95%) estimation. It sums up to a maximal error in volume accuracy of $\Delta V = \pm 8$ nl.

Beside the evaluation of the influence of the dielectric constant to the sensor performance, this experiment can also be seen as validation for (2), used as volume calibration equation for the sensor. Applying the identical calibration factors C_1 to C_3 as used in Section V, lead to a very good correlation of the droplet volumes measured by the sensor to the gravimetrically determined volumes. Thus, (2) including C_1 to C_3, defined in Section V, can be taken as precise volume calibration for the contactless measurement of dispensed droplets in the nanoliter range for the given sensor geometry. A further considerable influence parameter, which occurs in theory, is the droplet's lateral position in between the measurement capacitor electrodes.

Due to the inhomogeneity of the electric field in between the half shell electrodes (see Fig. 1), the specific position of a droplet relative to the capacitor's centre influences the magnitude of the change in capacitance. This can be simply deduced from Maxwell's first law. According to this, the influence of a dielectric body inserted into an electric field changes the flux density proportional to the electric field strength E [13].

$$\vec{D} = \vec{E} \cdot \varepsilon_0 \cdot \varepsilon_r. \tag{6}$$

From this it can be seen that an initially high flux density, influenced by a certain dielectric medium, increases significantly stronger than for an initially low flux density. Therefore, a droplet passing through a region of higher electrical field strength will lead to a larger change in flux density, thus to a larger change in capacity of the enclosing plate capacitor.

The experiment, presented in Section VI-B studied the influence of the lateral droplet position relative to the capacitor's center. Fig. 10 illustrates five analog sensor signals generated by droplets dispensed at similar parameters (velocity and volume) at five different lateral droplet positions within the measurement capacitor. It can be seen that the maximum peak signal value changes for the different positions. Droplets passing through regions with higher electrical field density, identified by finite element method (FEM) simulation, entail higher signal peak values.

Therefore, the experimental results are in agreement with theory. The error associated with this position dependency, when the calibrated sensor is used for volume measurements,

is in the worst case $\Delta V \sim 12$ nl, which corresponds to voltage variations of approximately $\Delta U = 100$ mV. Therefore, the flight path alignment has to be considered carefully when measuring droplet volumes, otherwise systematic errors in the mentioned order might occur.

VII. Conclusion

We presented a capacitive principle for the contactless measurement of the velocity and the volume of dispensed nanoliter droplets on the fly. An analog sensor signal generated by the presence of a liquid droplet in between the measurement capacitor comprehends variety information, enabling the determination of the droplet velocity and the droplet volume at once.

A calibration equation, (2), is deduced consistent of values which can be taken directly from a generated signal. The required calibration parameters are derived by standard multiple regression estimation. The application of this calibration equation combined with the presented sensor enables an accurate online measurement of the volumes of dispensed nanoliter droplets in the range from $V = \{26 - 82\,\text{nl}\}$ with an accuracy of $\Delta V = \pm 3$ nl. Also, the droplet velocity can be determined from the signals with a maximal deviation in accuracy of $\Delta u = +0.1$ m/s at a precision of $\Delta u = \pm 0.1$ m/s for the considered droplet velocity range ($u_{\text{droplet}} < 1.3$ m/s).

Furthermore, the influence of the media's dielectric constant on the capacitive measurement method turned out to be neglectable for dielectric constants in the range from $\varepsilon_r = \{43 \text{ to } 81\}$ by experiment; thus, it also agrees with theory.

Only the effect of the inhomogeneous electric field, caused by the half shell shape of the measurement capacitor's electrodes, leads to a sensitivity of the sensor signal to misalignments of the droplets flight path with respect to the center of the capacitor, which in the worst case might entail systematic measurement errors up to $\Delta V = 12$ nl.

The demonstrated performance of the presented droplet sensor discloses a new state-of-the-art method for noncontact process control for low-volume dispensing systems. The online measurement principle serves directly, after a droplet is ejected out of the nozzle, with quantitative values like the droplets velocity and volume. Therefore, a 100% process control can be realized, enabling to record the quality of a complete dispensing process without interfering with the dispensing performance or loss of media.

References

[1] Comley, "Continued miniaturisation of assay technologies drives market for NANOLITRE DISPENSING," *Drug Discovery World*, vol. Summer 2004, pp. 1–8, Jul. 2004.

[2] K. Thurow, T. Krüger, and N. Stoll, "An optical approach for the determination of droplet volumes in nanoliterdispensing," *J. Autom. Methods Manage. Chem.*, vol. 2009, Article ID 198732.

[3] J. Auge, K. Dierks, S. Prange, and B. Henning, "Monitoring of droplet growth with nano-litre resolution for liquid flow rate, level or surface tension measurement," *Sens. Actuators A-Phys.*, vol. 110, no. 1–3, pp. 18–27, Feb. 2004.

[4] W. Streule, T. Lindemann, G. Birkle, R. Zengerle, and P. Koltay, "PipeJet: A simple disposable dispenser for the nano- and microliter range," *J. Assoc. Lab. Automat.*, vol. 9, no. 5, pp. 300–306.

[5] A. Ernst, W. Streule, N. Schmitt, R. Zengerle, and P. Koltay, "A capacitive sensor for non- contact nanoliter droplets," *Sen. Actuators: A. Phys.2009*, no. Doi:10.1016/j.sna.2009.04.023, 2004.

[6] B. T. Williams, "Low Impedance Electrostatic Detector," U.S. Patent 4,370,616, 1983.

[7] R. J. Widlar, "IC Op Amp Beats FETs on Input Current," National Semiconductor, 2009, Application Note 29.

[8] BioFluidix GmbH. Freiburg, Germany. [Online]. Available: http://www.biofluidix.de

[9] A. Ernst, W. Streule, R. Zengerle, and P. Koltay, "Quantitative volume determination of dispensed nanoliter droplets on the fly," in *Proc. Transducers'09*, Denver, CO, 2009, pp. 1750–1753.

[10] IDS imaging development systems GmbH. Obersulm, Germany. [Online]. Available: http://www.ids-imaging.com

[11] A. Horibe, S. Fukusako, and M. Yamba, "Surface tension of low-temperature aqueous solutions," *Int. J. Thermophys.*, vol. 17, no. 2, 1996.

[12] J. A. Lane and J. A. Saxton, "Dielectric dispersion in pure polar liquids at very high radio frequencies," in *Proc. R. Soc. London*, 1952, Series A, Math. and Phys. Sci.

[13] J. D. Jackson, *Classical Electrodynamics*, 3rd ed. New York: Wiley, 1998.

Andreas Ernst was born in Bad Säckingen, Germany, in 1976. He received the diploma degree in medical engineering from the University of Applied Science of Furtwangen, Schwenningen, Germany. He is currently working towards the Ph.D. degree at the Laboratory for MEMS Applications, Department of Microsystems Engineering (IMTEK), University of Freiburg, Freiburg, Germany.

His research interest includes the development of direct quality control systems for pipetting and noncontact dispensing systems.

Lin Ju received the B.Eng. degree in industrial automation from Qingdao University, Qingdao, China, in 2000 and the M.Sc. degree from Hochschule Darmstadt University of Applied Sciences, Darmstadt, Germany, in 2007.

After the B.Eng. degree, she was with Sinopec China as an Electrical Engineer. She is currently a Research Assistant at the faculty of Mechanical and Process Engineering, Hochschule Furtwangen University, Schwenningen, Germany. Her current areas of interest include sensor technology and signal processing.

Bernhard Vondenbusch studied electrical engineering and received the Ph.D. degree from the Technical University of Aachen, Aachen, Germany, in 1988.

Afterwards, he joined the Helmholtz-Institute for Biomedical Engineering, Aachen, and worked in the field of acquisition and digital processing of multiple biosignals. He then spent several years in the aircraft industry and joined the University of Applied Sciences of Furtwangen, Schewnningen, Germany, in 1993. He is now head of the degree course Medical Engineering and gives lectures in electronics, control system theory, digital signal processing, and medical sensors. He also is Director of the Steinbeis Transfer Center Biomedical Engineering, which was founded in 1994. The STC Biomedical Engineering supports the medical industry in research and development of medical devices as well as in regulatory affairs. His research interests are focused on the delivery of high-energy radiation to the skin and on transdermal drug delivery systems.

Roland Zengerle is the Director of the Department of Microsystems Engineering (IMTEK), University of Freiburg, Freiburg, Germany. He also heads the Laboratory for MEMS Applications at IMTEK and in addition he is a Director at the Institute for Micro- and Information Technology of the Hahn-Schickard-Gesellschaft (HSG-IMIT). HSG-IMIT is a nonprofit organization supporting industries in development of new products based on MEMS technologies. His research is focused on microfluidics and covers topics like miniaturized and autonomous dosage systems, implantable drug delivery systems, nanoliter and picoliter dispensing, lab-on-a-chip platforms, tools for research on cells, thermal sensors, miniaturized fuel cells, as well as micro- and nanofluidics simulation. Dr. Zengerle coauthored more than 300 technical publications and 30 patents. He is the European editor of the *Springer Journal of Microfluidics and Nanofluidics*.

Dr. Zengerle serves on the international steering committee of the IEEE-MEMS conference as well as on the technical program committees of several other international conferences.

Peter Koltay studied physics at the University of Freiburg, Freiburg, Germany, and the University of Budapest, Budapest, Hungary, and received the Ph.D. degree from the University of Freiburg in 1999.

Afterwards, he joined the laboratory of Prof. Zengerle at the Institute for Microsystem Technology (IMTEK), University of Freiburg, as a Faculty Member. In 2005, he founded the company BioFluidix GmbH to commercialize noncontact dispensing technologies developed at IMTEK. His research interests are especially related to the development of noncontact liquid-handling technologies, sensors for droplet detection and quality control, modeling of droplet and bubble dynamics, design and fabrication of passive direct methanol fuel cells, and simulation of microfluidic devices by numerical methods.